

# Detection of evolutionary shifts in variance under an Ornstein–Uhlenbeck model

Wensha Zhang<sup>1</sup>, Lam Si Tung Ho<sup>2\*</sup>, Toby Kenney<sup>3\*</sup>

April 1, 2025

<sup>1,2,3</sup>Department of Mathematics and Statistics, Dalhousie University, Nova Scotia, Canada

\*These authors have equal contribution

E-mails: {wn209685, Lam.Ho, tb432381}@dal.ca

## Abstract

Abrupt environmental changes can lead to evolutionary shifts in not only the optimal trait value ( $\theta$ ), but also the rate of adaptation ( $\alpha$ ) and the diffusion variance ( $\sigma^2$ ) in trait evolution. While several methods exist for detecting shifts in optimal values, few explicitly model shifts in both evolutionary variance and adaptation rates. We use a multi-optima and multi-variance Ornstein-Uhlenbeck (OU) process model (Beaulieu, Jhwueng, Boettiger, and O’Meara, 2012) to describe trait evolution with shifts in both  $\theta$  and  $\sigma^2$  and analyze how covariance between species is affected when shifts in variance occur along the phylogeny. We propose a new method that simultaneously detects shifts in both variance and optimal values by formulating the problem as a variable selection task using an  $\ell_1$ -penalized loss function. Our method is implemented in the R package `ShiVa` (Detection of evolutionary shifts in variance). Through simulations, we compare `ShiVa` with methods that only consider shifts in optimal values (`ℓ1ou`; `PhylogeneticEM`). Our method demonstrates improved predictive ability and significantly reduces false positives in detecting optimal value

shifts when variance shifts are present. When only shifts in optimal value occur, our method performs comparably to existing approaches. Applying **ShiVa** to empirical data from cordylid lizards (Broeckhoven, Diedericks, Hui, Makhubo, and Mouton, 2016a), we find that it outperforms  $\ell_{1ou}$  and PhylogeneticEM, achieving the highest log-likelihood and lowest BIC. evolutionary shift detection, Ornstein-Uhlenbeck model, LASSO, trait evolution, phylogenetic comparative methods

## 1 Introduction

The process of trait evolution is influenced by environmental conditions. When species experience abrupt environmental changes, their evolutionary processes may also change to adapt to the new environment (Losos, 2011; Mahler, Ingram, Revell, and Losos, 2013a). These changes in the evolutionary process leave signatures in the observed traits of present-day species. By detecting such evolutionary shifts based on observed trait data, we gain valuable insights into historical environmental changes and the evolutionary history of species.

To model the evolutionary process along a phylogenetic tree, researchers commonly use two statistical frameworks: the Brownian Motion (BM) model (Felsenstein, 1985) and the Ornstein-Uhlenbeck (OU) process model (Hansen, 1997). Evolutionary shifts are typically modeled as changes in the parameters of these processes. Much of the existing research focuses on detecting shifts in the current value (under BM) or shifts in the optimal trait value (under OU). Butler and King [2004] formulated the multiple-optima OU model, which allows shifts in the selective optima across different branches of a phylogeny and detects these shifts using hypothesis testing. Uyeda and Harmon [2014] introduced a Bayesian framework to detect such shifts in selective optima. Ho and Ané [2014] highlighted limitations of using AIC and BIC in shift detection tasks, proposing a modified BIC and a forward-backward model selection procedure. Khabbazian et al. [2016] treated the shift detection problem as a variable selection task, applying LASSO to detect shifts in

selective optima, implemented in the *ℓ1ou* R package. This LASSO-based approach enables efficient shift detection, and they further proposed a new information criterion (pBIC) to account for phylogenetic correlations. Other methods, such as PhylogeneticEM (Bastide, Mariadassou, and Robin, 2017), apply expectation-maximization (EM) to estimate shifts in the optima. Zhang et al. [2024] extended this line of work with the ELPASO package, which uses ensemble variable selection to improve robustness under model violations. However, these methods primarily focus on detecting shifts in optimal values and do not explicitly detect the shifts in evolutionary diffusion variance. In reality, abrupt environmental changes are likely to influence not only the optimal trait values but also the evolutionary variance, which reflects how much random fluctuation occurs around the evolutionary process. In this paper, the term variance specifically refers to the diffusion variance ( $\sigma^2$ ), which quantifies the background rate of stochastic variation in trait evolution. This variance may increase under unstable environments or decrease under stabilizing conditions. Some existing methods allow modeling shifts in evolutionary parameters, including the optimal value ( $\theta$ ), the rate of adaptation ( $\alpha$ ) and the evolutionary variance ( $\sigma^2$ ). Pagel and Meade [2006] introduced BayesTraits, which allows shifts in both optimal values and rates of evolution (modeled as  $\alpha$ ). Beaulieu et al. [2012] developed the OUwie package, which supports detecting shifts in both optimal values and the rate of adaptation across branches in the tree. Later, Clavel et al. [2015] introduced mvMorph, which extends evolutionary modeling to multivariate traits, allowing shifts in both the rate of adaptation and evolutionary variance across lineages. More recently, Bastide et al. [2021] developed a flexible Bayesian framework using Hamiltonian Monte Carlo (HMC) sampling, which supports models with shifting evolutionary variances. Finally, Mitov et al. [2020] proposed the  $\mathcal{G}_{LInv}$  family of Gaussian phylogenetic models, providing an efficient likelihood-based approach to model variance shifts across branches.

While these tools allow evolutionary shifts to be modeled, they typically require either pre-specified regimes or rely on computationally intensive full Bayesian inference. Further-

more, few methods explicitly focus on detecting both shifts in optimal value and shifts in variance simultaneously using a data-driven variable selection framework. In this paper, we propose a novel LASSO-based method that detects both types of shifts within a unified variable selection framework. Our method uses a multi-optima and multi-variance OU process model, similar to the models used in OUwie (Beaulieu, Jhwueng, Boettiger, and O’Meara, 2012), but innovates by formulating the detection of both shifts in optima and shifts in variance as a single variable selection problem, solvable using LASSO. This approach allows flexible and efficient detection of shifts across the entire tree, without requiring a *priori* specification of regime boundaries.

We implement this approach in a new R package, **ShiVa** (Detection of Evolutionary Shifts in Variance). Through simulation studies, we compare **ShiVa** to existing methods, including *ℓ1ou* and PhylogeneticEM, evaluating performance in terms of both shift detection accuracy and predictive performance.

The remainder of the paper is organized as follows. The *Trait evolution with shifts in both optimal value and variance* section introduces the trait evolution model incorporating shifts in both optimal value and variance, and formally defines the shift detection problem. The *Methods* section describes the LASSO-based shift detection algorithm. The *Simulations* section presents simulation results, including comparisons with existing methods. The *Case study* section illustrates the application of **ShiVa** to empirical data from cordylid lizards (Broeckhoven, Diedericks, Hui, Makhubo, and Mouton, 2016a). *Conclusion* concludes with a discussion of the advantages, limitations, and potential extensions of the method.

## 2 Trait evolution with shifts in both optimal value and variance

### 2.1 Trait evolution models

The phylogenetic tree is reconstructed from DNA sequences and is assumed to be known in this paper. The phylogenetic tree reveals the correlation structure between trait values of different species. The trait values are correlated based on the shared evolutionary history of species. The trait values of internal nodes are hidden and only trait values of tip nodes can be observed. When  $\alpha$  is unknown, a reasonable estimate can be obtained by fitting a null model (a model without shifts) using the `phylolm` package. Throughout this paper, we focus on estimating the parameters related to shifts, while the trait values of internal nodes remain hidden and only the trait values at the tips of the tree are observed. Trait evolution models are used to model how the trait values change over time. Brownian Motion and Ornstein–Uhlenbeck are two commonly used models to model the evolution of continuous traits. The BM model is a special case of the OU model. For both models, we let  $Y$  denote the vector of observed trait values at the tips, and  $Y_i$  denote the trait value of taxon  $i$ . For a single branch, we let  $Y_i(t)$  denote the trait value at time  $t$ . These two models assume that conditioning on the trait value of a parent, the evolutionary processes of sister species are independent. We therefore only need to specify the model on one branch. For specifying the model on a single branch, we let  $Y(t)$  denote the trait value at time  $t$  on a fixed branch.

#### Brownian Motion Model

Brownian motion (BM) was first applied to model the evolution of continuous traits over time by Felsenstein [1985]. Under this model, the trait value evolves following a BM pro-

cess. The process can be written as a stochastic differential equation:

$$dX_t = \sigma(t) dW_t,$$

where  $\sigma^2(t)$  is the instantaneous diffusion variance at time  $t$ , and  $W_t$  is a standard Wiener process. The evolution processes of two species are independent, given the trait value of their most recent common ancestor. Therefore, the correlation between the trait values of two species depends only on the evolution time they shared. Based on the properties of the BM process, the observed trait values  $Y$  follow a multivariate Gaussian distribution. For an ultrametric tree of height 1, each  $y_i$  has mean  $\mu_0$  and variance at time  $t$ ,  $\sigma^2(t)$ , so the covariance between  $y_i$  and  $y_j$  is  $\int_0^{t_{ij}} \sigma^2(t) dt$ , where  $t_{ij}$  is the shared evolution time between species  $i$  and  $j$ .

### Ornstein–Uhlenbeck Model

[Hansen, 1997] uses an OU process to model the evolutionary process. A selection force that pulls the trait value toward a selective optimum  $\theta$  is included in OU models. An OU process  $Y(t)$  is defined by the following stochastic differential equation

$$dY(t) = \alpha[\theta(t) - Y(t)]dt + \sigma(t)dB(t)$$

where  $dY(t)$  is the infinitesimal change in trait value;  $B(t)$  is a standard BM;  $\sigma^2(t)$  measures the intensity of random fluctuation at time  $t$ ;  $\theta(t)$  is the optimal value of the trait at time  $t$ ; and  $\alpha \geq 0$  is the selection strength. When  $\alpha = 0$ , the OU process is the same as a BM. We assume that  $\alpha$  is constant. For the BM model, the variance of the trait  $\int_0^T \sigma^2(t) dt$  is unbounded when  $T$  increases. On the other hand, for the OU model, the variance of the trait  $\int_0^T \sigma^2(t) e^{-2\alpha(T-t)} dt$  is bounded, which is considered more realistic for most traits. Therefore, compared to the BM model, the OU model is often preferred for modeling the evolutionary process.

## 2.2 Evolutionary shifts in optimal value and variance

Butler and King [2004] formulate the multi-optima OU model for adaptive evolution. This model assumes that the optimal value  $\theta(t)$  is constant along a branch and may be different between branches. An abrupt change in  $\theta(t)$  on a branch is considered an evolutionary shift in optimal value. However, in most previous work, it is assumed that the variance  $\sigma^2(t)$  is constant throughout the tree. In reality, when a change in the environment happens, not only the optimal values, but also the variances are likely to change. In this paper, we use a multi-optima multi-variance model (Beaulieu, Jhwueng, Boettiger, and O'Meara, 2012) which allows the variances  $\sigma(t)$  to change over different branches.

Solving the OU process equation, the trait value at time  $t$  is given by

$$Y_t = y_0 e^{-\alpha t} + \alpha \int_0^t e^{-\alpha(t-s)} \theta(s) ds + \int_0^t \sigma(s) e^{-\alpha(t-s)} dW_s$$

Solving this, the trait value of species  $i$  follows a normal distribution with expectation given by:

$$E(Y_i) = y_0 e^{-\alpha T} + \alpha \int_0^T e^{-\alpha(T-s)} \theta(s) ds$$

By Itô isometry, the element  $\Sigma_{i,j}$  (covariance of  $Y_i$  and  $Y_j$ ) of covariance matrix  $\Sigma$  is given by

$$\Sigma_{i,j} = e^{-2\alpha(T-t_a)} \int_0^{t_a} \sigma^2(s) e^{-2\alpha(t_a-s)} ds$$

Where  $a$  is the separating point of species  $i$  and  $j$ . For ultrametric trees, the distance between  $i$  and  $j$  is  $2t_{ai} = 2t_{aj} = 2(T - t_a)$ . For shifts in optimal value, Ho and Ané [2014] showed that the exact location and number of shifts on the same branch are unidentifiable. We therefore also assume that the optimal value is constant along a branch. We let  $\theta_b$  denote the optimal value on branch  $b$ ,  $\Delta\theta_b$  denote the change in optimal value on branch  $b$

and  $\text{path}(\text{root}, i)$  denote the branches on the path of the phylogenetic tree from the root to the tip  $i$ . The expectation can be written as the following equation (Khabbazian, Kriebel, Rohe, and Ané, 2016).

$$E(Y_i) = y_0 e^{-\alpha T} + (1 - e^{-\alpha T})\theta_0 + \sum_{b \in \text{path}(\text{root}, i)} (1 - e^{-\alpha t_b})\Delta\theta_b$$

Let  $\beta_0 = y_0 e^{-\alpha T} + (1 - e^{-\alpha T})\theta_0$  and  $\beta_b = (1 - e^{-\alpha t_b})\Delta\theta_b$ . Then,

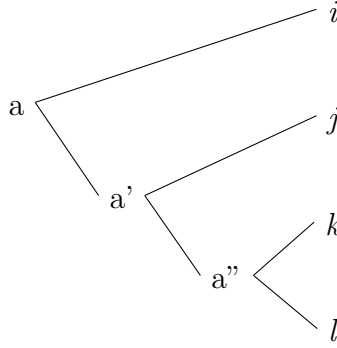
$$E(Y_i) = \beta_0 + \sum_b \beta_b \mathbf{X}_{bi} \tag{1}$$

where  $X_b$  is a vector defined by  $X_{bi} = 0$  if taxon  $i$  is not under branch  $b$ , and  $X_{bi} = 1$  if the taxon  $i$  is under branch  $b$ .

While shifts in optimal value only affect the expectation of the  $Y_i$ , shifts in variance affect the variance of  $Y_i$  and the covariance of  $Y_i$  and  $Y_j$ . In particular, if species  $i$  and  $j$  separate at time  $t_a$ , and the shifts in variance along the shared evolutionary path occur at times  $t_1, \dots, t_m$ , with magnitudes  $\Delta\sigma_1^2, \Delta\sigma_2^2, \dots, \Delta\sigma_m^2$  respectively, then the covariance  $\Sigma_{ij}$  is given by

$$\Sigma_{i,j} = \frac{e^{-2\alpha(T-t_a)}}{2\alpha} \left( (1 - e^{-2\alpha t_a})\sigma_0^2 + \sum_{l \in \text{path}(\text{root}, a)} (1 - e^{-2\alpha(t_a-t_l)}) \Delta\sigma_l^2 \right)$$

The results of Ho and Ané [2014] about the unidentifiability of shift positions along a branch are not completely applicable for shifts in variance. By examining the covariance between pairs of species under a given branch, we can estimate the covariance at the end of the branch, and from their mean, we can estimate the trait value at the end of the branch. This can result in different likelihoods for different positions of a single shift on a branch, so the position is identifiable. For example, considering the species  $i, j, k, l$  on the following tree:



With a single shift in variance on the branch from a to a', we have the following equations to solve for the time and magnitude of the shift.

$$\begin{aligned} \Sigma_{jk} - \Sigma_{ij} &= \sigma_0^2/2\alpha(e^{-2\alpha(T-t_{a'})} - e^{-2\alpha(T-t_a)}) + \Delta\sigma^2/2\alpha(e^{-2\alpha(T-t_{a'})} - e^{-2\alpha(T-t_a)}) \\ \Sigma_{kl} - \Sigma_{jk} &= \sigma_0^2/2\alpha(e^{-2\alpha(T-t_{a''})} - e^{-2\alpha(T-t_{a'})}) + \Delta\sigma^2/2\alpha(e^{-2\alpha(T-t_{a''})} - e^{-2\alpha(T-t_{a'})}) \end{aligned}$$

which can easily be seen to be solveable for both  $\Delta\sigma^2$  and  $t$ . However, the times, magnitudes and even number of shifts will be unidentifiable if there are two (or more) shifts on the same branch. For example, if there are shifts in variance at times  $t_1$  and  $t_2$  on branch  $b$ , with magnitudes  $\Delta\sigma_1^2$  and  $\Delta\sigma_2^2$  respectively, then for any two species below branch  $b$ , their covariance will include the term  $\frac{e^{-2\alpha(T-t_a)}}{2\alpha} (1 - e^{-2\alpha(t_a-t_1)}) \Delta\sigma_1^2 + \frac{e^{-2\alpha(T-t_a)}}{2\alpha} (1 - e^{-2\alpha(t_a-t_2)}) \Delta\sigma_2^2$ . Thus it is not possible to separate  $\Delta\sigma_1^2$  and  $\Delta\sigma_2^2$ , or  $t_1$  and  $t_2$ . Indeed, in many cases, there is a single shift on branch  $b$  that would produce the same covariance matrix.

For model and computational simplicity, we assume that  $\sigma^2$  is constant over a branch like the assumption for  $\theta$ . That is, we assume that any shift in variance on a branch occurs at the beginning of that branch. For shifts in mean, this assumption did not limit the space of possible models due to the unidentifiability. However, for shifts in variance, this does restrict the space of models for the trait values at the leaves, and could therefore adversely affect shift detection. We will study whether this adverse effect is cause for concern in our simulation studies.

Under our assumptions, we let  $\sigma_b^2$  denote the variance on the branch  $b$ ,  $\Delta\sigma_b^2$  denote the magnitude of shift in variance on the branch  $b$ : if no shift occurs on the branch  $b$ ,  $\Delta\sigma_b^2 = 0$ . The covariance between species  $i$  and  $j$  is given by:

$$\begin{aligned}
 \Sigma_{i,j} &= \frac{e^{-2\alpha(T-t_a)}}{2\alpha} \left( (1 - e^{-2\alpha t_a})\sigma_0^2 + \sum_{b \in \text{path}(\text{root}, a)} (1 - e^{-2\alpha(t_a - t_b)})\Delta\sigma_b^2 \right) \\
 &= \frac{e^{-2\alpha(T-t_a)}}{2\alpha} \left( (1 - e^{-2\alpha t_a})\sigma_0^2 + \sum_{b \in \text{path}(\text{root}, a)} (1 - e^{-2\alpha t_a} + e^{-2\alpha t_a} - e^{-2\alpha(t_a - t_b)}) \Delta\sigma_b^2 \right) \\
 &= \frac{e^{-2\alpha(T-t_a)}}{2\alpha} \left( (1 - e^{-2\alpha t_a})\sigma_0^2 + \sum_{b \in \text{path}(\text{root}, a)} ((1 - e^{-2\alpha t_a}) + e^{-2\alpha t_a}(1 - e^{2\alpha t_b})) \Delta\sigma_b^2 \right) \\
 &= \frac{e^{-2\alpha(T-t_a)}}{2\alpha} (1 - e^{-2\alpha t_a}) \sigma_0^2 + \sum_{b \in \text{path}(\text{root}, a)} \frac{e^{-2\alpha(T-t_a)}}{2\alpha} (1 - e^{-2\alpha t_a}) \Delta\sigma_b^2 \\
 &\quad + \sum_{b \in \text{path}(\text{root}, a)} \frac{e^{-2\alpha T}}{2\alpha} (1 - e^{2\alpha t_b}) \Delta\sigma_b^2 \tag{2}
 \end{aligned}$$

For the ancestral state at the root node, two different assumptions are commonly used, fixed value or stationary distribution. We assume that the ancestral state at the root is a fixed value for the above process. Equation 2 is the covariance of node  $i$  and  $j$  for the OU model with fixed root. For the OU model, the ancestral state at the root is also often assumed to have the stationary distribution. In this case, the covariance of the root node

is  $\sigma_0^2/(2\alpha)$  (Ho and Ané, 2013). In this case, the covariance with shifts can be written as:

$$\begin{aligned}\Sigma_{i,j} &= \frac{e^{-2\alpha(T-t_a)}}{2\alpha} (1 - e^{-2\alpha t_a}) \sigma_0^2 + \sum_{b \in \text{path}(\text{root}, a)} \frac{e^{-2\alpha(T-t_a)}}{2\alpha} (1 - e^{-2\alpha t_a}) \Delta\sigma_b^2 \\ &\quad + \sum_{b \in \text{path}(\text{root}, a)} \frac{e^{-2\alpha T}}{2\alpha} (1 - e^{2\alpha t_b}) \Delta\sigma_b^2 + \frac{e^{-2\alpha T}}{2\alpha} \sigma_0^2 \\ &= \frac{e^{-2\alpha(T-t_a)}}{2\alpha} \sigma_0^2 + \sum_{b \in \text{path}(\text{root}, a)} \frac{e^{-2\alpha(T-t_a)}}{2\alpha} (1 - e^{-2\alpha t_a}) \Delta\sigma_b^2 \\ &\quad + \sum_{b \in \text{path}(\text{root}, a)} \frac{e^{-2\alpha T}}{2\alpha} (1 - e^{2\alpha t_b}) \Delta\sigma_b^2\end{aligned}$$

Let  $\gamma_b = \Delta\sigma_b^2$ ,  $\mathbf{V}_{i,j} = \frac{e^{-2\alpha(T-t_a)}}{2\alpha} (1 - e^{-2\alpha t_a})$ ,  $\mathbf{U}_{i,j} = \frac{e^{-2\alpha(T-t_a)}}{2\alpha}$ ,  $q_b = \frac{e^{-2\alpha T}}{2\alpha} (1 - e^{2\alpha t_b})$ ;  $\gamma_b$  is the shift in variance on branch  $b$ ,  $\mathbf{V}$  is the phylogenetic covariance matrix when  $\sigma^2 = 1$  (no shift in variance) with fixed root,  $\mathbf{U}$  is the phylogenetic covariance matrix when  $\sigma^2 = 1$  (no shift in variance) with stationary distributed root.  $\mathbf{U}$  and  $\mathbf{V}$  only depend on the phylogeny. The covariance between species  $i$  and  $j$  can be expressed as the following equation.

$$\Sigma_{i,j} = \begin{cases} \mathbf{V}_{i,j} \sigma_0^2 + \sum_b \gamma_b X_{ib} X_{jb} \mathbf{V}_{i,j} + \sum_b \gamma_b q_b X_{ib} X_{jb} & \text{OU model with fixed root} \\ \mathbf{U}_{i,j} \sigma_0^2 + \sum_b \gamma_b X_{ib} X_{jb} \mathbf{V}_{i,j} + \sum_b \gamma_b q_b X_{ib} X_{jb} & \text{OU model with random root} \end{cases}$$

It consists of 3 terms. The first term is the original covariance without any shift. The last 2 terms show the influence of shifts in variances. In addition to the shift sizes  $\gamma_b$ , the second term is influenced by the phylogentic structure ( $\mathbf{V}_{i,j}$ ), higher original covariance between two species leads to larger change in covariance for a fixed shift size (Fig. 1); the third term is influenced by the start time of branch  $b$  ( $q_b$ ), earlier shifts lead to larger change in covariance between two species (Fig. 2).

For simplicity, we let  $\mathbf{R}$  denote the phylogenetic covariance matrix when there is no shift in variance and  $\sigma_0^2 = 1$ . So  $\mathbf{R} = \mathbf{V}$  when the root is fixed and  $\mathbf{R} = \mathbf{U}$  when the trait value at the root follows the stationary distribution.

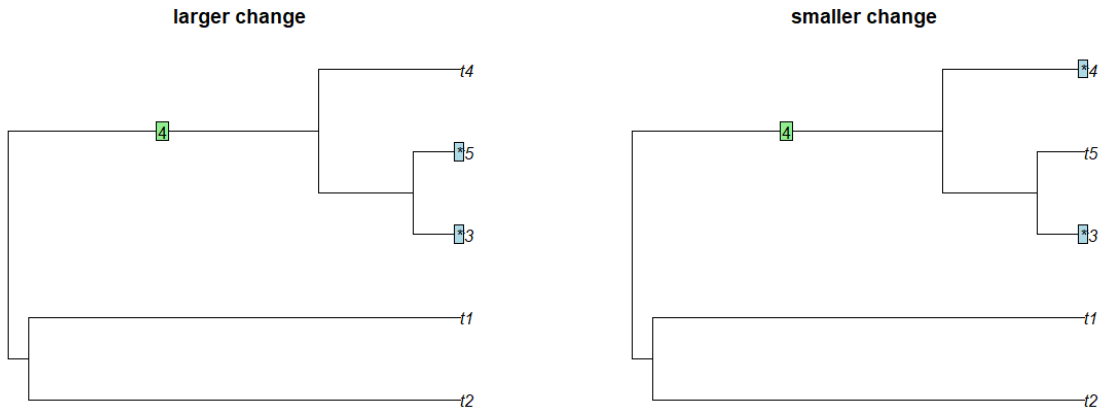


Figure 1: Higher original covariance between two species leads to larger change in covariance for the same shift magnitude: larger change for the shift in the left figure

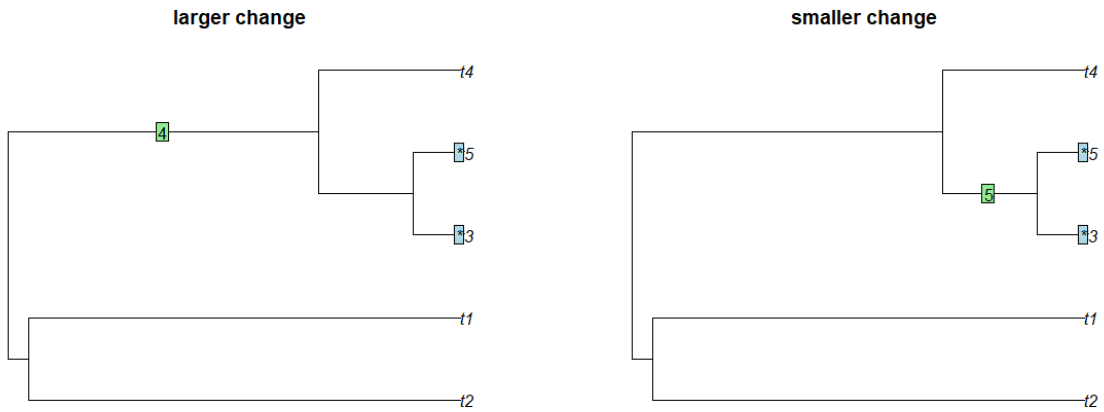


Figure 2: Earlier shift leads to larger change in covariance for a given species: larger change for the shift in the left figure

Using matrix notation, the covariance matrix can be expressed as:

$$\begin{aligned}\boldsymbol{\Sigma} &= \sigma_0^2 \mathbf{R} + \left( \sum_{b=1}^p \gamma_b \mathbf{X}_b \mathbf{X}_b^T \right) \odot \mathbf{V} + \sum_{b=1}^p \gamma_b q_b \mathbf{X}_b \mathbf{X}_b^T \\ &= \sigma_0^2 \mathbf{R} + (\mathbf{X} \text{diag}(\boldsymbol{\gamma}) \mathbf{X}^T) \odot \mathbf{V} + \mathbf{X} \text{diag}(\boldsymbol{\gamma} \odot \mathbf{q}) \mathbf{X}^T\end{aligned}\quad (3)$$

Where  $\odot$  represents elementwise multiplication of matrices and vectors. The trait values at tips can be written as:

$$\mathbf{Y} = \beta_0 \mathbf{1} + \sum_b \beta_b \mathbf{X}_b + \epsilon$$

Where  $\epsilon$  follows a normal distribution with mean 0 and covariance matrix  $\boldsymbol{\Sigma}$ , given by Equation 3. The main task is to select the branches that have  $\beta_b \neq 0$  and  $\gamma_b \neq 0$ ; and estimate the values of  $\beta_b$  and  $\gamma_b$ .

### 3 Methods

In this section, we propose a new method to simultaneously detect the shifts in both variance and optimal values based on minimizing the loss function with L1 penalty. When  $\mathbf{Y}$  follows a multivariate normal distribution with mean and variance given by Equations 1 and 3, the log likelihood is

$$\begin{aligned}L(\boldsymbol{\beta}, \boldsymbol{\gamma}) &= -\frac{1}{2}(\mathbf{Y} - \beta_0 - \mathbf{X}\boldsymbol{\beta})^T \boldsymbol{\Sigma}^{-1}(\mathbf{Y} - \beta_0 - \mathbf{X}\boldsymbol{\beta}) - \frac{1}{2} \log \det(\boldsymbol{\Sigma}) \\ &= -\frac{1}{2}(\mathbf{Y} - \beta_0 - \mathbf{X}\boldsymbol{\beta})^T (\sigma_0^2 \mathbf{R} + (\mathbf{X} \text{diag}(\boldsymbol{\gamma}) \mathbf{X}^T) \odot \mathbf{V} + \mathbf{X} \text{diag}(\boldsymbol{\gamma} \odot \mathbf{q}) \mathbf{X}^T)^{-1} (\mathbf{Y} - \beta_0 - \mathbf{X}\boldsymbol{\beta}) \\ &\quad - \frac{1}{2} \log \det(\sigma_0^2 \mathbf{R} + (\mathbf{X} \text{diag}(\boldsymbol{\gamma}) \mathbf{X}^T) \odot \mathbf{V} + \mathbf{X} \text{diag}(\boldsymbol{\gamma} \odot \mathbf{q}) \mathbf{X}^T)\end{aligned}$$

To select the shifts in optimal values ( $\beta_i \neq 0$ ) and the shifts in variances ( $\gamma_i \neq 0$ ), we use an L1 penalty in the loss function to conduct the feature selection as in LASSO. There-

fore, the loss function to be optimized is given by:

$$\begin{aligned}
 L(\beta_1, \dots, \beta_p, \gamma_1, \dots, \gamma_p) &= l(\beta_1, \dots, \beta_p, \gamma_1, \dots, \gamma_p; \mathbf{Y}) + \text{Penalty} \\
 &= \frac{1}{2}(\mathbf{Y} - \beta_0 - \mathbf{X}\beta)^T \left( \sigma_0^2 \mathbf{R} + \left( \sum_{i=1}^p \gamma_i \mathbf{X}_i \mathbf{X}_i^T \right) \odot \mathbf{V} + \sum_{i=1}^p \gamma_i q_i \mathbf{X}_i \mathbf{X}_i^T \right)^{-1} \\
 &\quad (\mathbf{Y} - \beta_0 - \mathbf{X}\beta) + \frac{1}{2} \log \det \left( \sigma_0^2 \mathbf{R} + \left( \sum_{i=1}^p \gamma_i \mathbf{X}_i \mathbf{X}_i^T \right) \odot \mathbf{V} + \sum_{i=1}^p \gamma_i q_i \mathbf{X}_i \mathbf{X}_i^T \right) \\
 &\quad + \lambda_1 \|\beta\|_1 + \lambda_2 \|\gamma\|_1 \tag{4}
 \end{aligned}$$

### 3.1 Optimization

In this paper, we do not estimate the parameter  $\alpha$  jointly with other parameters, but instead treat it as fixed using an ad-hoc estimate obtained from the null model fitted by the `phylo1m` R package. Therefore, in this section, we treat it as fixed during the model fitting process. In the simulations, we demonstrate that the estimation of  $\alpha$  does not significantly affect the detection results. Therefore, we omit the estimation of  $\alpha$  in the ShiVa procedure. In cases where  $\alpha$  is unknown, we use an ad-hoc estimate of  $\alpha$  provided by fitting a null model (a model without shifts) using the `phylo1m` package. This estimated  $\alpha$  is then fixed when running ShiVa. The primary objective here is to find the parameters  $\beta$ ,  $\gamma$ , and  $\sigma_0^2$  that minimize the loss function described in Equation 4. When  $\gamma$  is fixed, the problem reduces to a standard LASSO formulation, which can be efficiently solved.

For optimizing  $\gamma$ , we employ coordinate-wise proximal gradient descent, as described by Parikh and Boyd [2014]. The proximal gradient algorithm is a powerful tool for handling non-differentiable convex optimization problems. It decomposes the objective function into two components: a differentiable part and a non-differentiable part, allowing for iterative updates that combine gradient descent with the proximal operator. The proximal operator serves to handle the non-differentiable component, promoting sparsity and effectively reducing the influence of irregularities in the model. By applying the proximal gradient

algorithm in our optimization process, we can efficiently minimize the objective function even when the problem involves non-smooth terms, such as LASSO regularization.

The loss function for  $\gamma_k$  can be written as:

$$L(\gamma_k) = g(\gamma_k) + \lambda_2 \|\gamma_k\|_1.$$

The derivative of  $g(\gamma_k)$  is given by:

$$\begin{aligned} (\nabla g(\gamma))_k &= -\frac{1}{2} \mathbf{r}^T \boldsymbol{\Sigma}^{-1} ((\mathbf{X}_k \mathbf{X}_k^T) \odot \mathbf{V}) \boldsymbol{\Sigma}^{-1} \mathbf{r} - \frac{1}{2} q_k \|\mathbf{X}_k^T \boldsymbol{\Sigma}^{-1} \mathbf{r}\|^2 + \frac{1}{2} \text{tr}(((\mathbf{X}_k \mathbf{X}_k^T) \odot \mathbf{V}) \boldsymbol{\Sigma}^{-1}) \\ &\quad + \frac{1}{2} q_k \mathbf{X}_k^T \boldsymbol{\Sigma}^{-1} \mathbf{X}_k, \end{aligned}$$

where  $\mathbf{r} = \mathbf{Y} - \beta_0 - \mathbf{X}^T \beta$ . The proximal operator is given by:

$$\text{prox}_{\lambda_2 h}(z) = S_{\lambda_2}(z) = \begin{cases} z - \lambda_2 & z > \lambda_2, \\ 0 & -\lambda_2 \leq z \leq \lambda_2, \\ z + \lambda_2 & z < -\lambda_2. \end{cases}$$

The proximal algorithm here steps in the direction  $\nabla g(\gamma)$  but setting any values that are close to zero equal to zero. For  $\sigma_0^2$ , there is no penalty on the parameter. Therefore, we use gradient descent to update  $\sigma_0^2$ . To avoid negative values of  $\sigma_0^2$ , we use  $\tau_0 = \log(\sigma_0^2)$  for optimization. The gradient of  $\tau_0$  is given by:

$$\frac{\partial L}{\partial \tau} = \left( -\frac{1}{2} \mathbf{r}^T \boldsymbol{\Sigma}^{-1} \mathbf{R} \boldsymbol{\Sigma}^{-1} \mathbf{r} + \frac{1}{2} \text{tr}(\mathbf{R} \boldsymbol{\Sigma}^{-1}) \right) e^{\tau_0}.$$

We initialize  $\beta$  and  $\gamma$  as 0. In each iteration, we first update the covariance matrix  $\boldsymbol{\Sigma}$  and transform  $\mathbf{X}$  and  $\mathbf{Y}$  with the current  $\boldsymbol{\Sigma}^{-1/2}$ . Then we update  $\beta$  by applying LASSO on the transformed data. Then we update  $\gamma$  using the proximal algorithm in an elementwise manner. After that, we update  $\tau_0^2$  using gradient descent. The algorithm is summarized in

Algorithm 1.

---

**Algorithm 1** Optimization with  $\beta$ ,  $\gamma$  and  $\tau_0$

---

```

1: Inputs:
    $M$ : maximum number of steps;  $t$ : step size;  $\epsilon$ : error tolerance;  $\mathbf{V}$ ;  $\mathbf{R}$ ;  $\mathbf{Y}$ ;  $\mathbf{X}$ ;  $\lambda_2$ 
2: Initialize:
    $\beta_i^0 \leftarrow 0, i = 1, \dots, p$ 
    $\gamma_i^0 \leftarrow 0, i = 1, \dots, p$ 
    $\tau_0 \leftarrow 0$ 
    $L \leftarrow Inf$ 
3: for  $s = 1$  to  $M$  do
4:    $\Sigma \leftarrow e^{(\tau_0)} \mathbf{R} + (\sum_{i=1}^p \gamma_i \mathbf{X}_i \mathbf{X}_i^T) \odot \mathbf{V} + \sum_{i=1}^p \gamma_i q_i \mathbf{X}_i \mathbf{X}_i^T$ 
5:    $\mathbf{Y}' = \Sigma^{-1/2} \mathbf{Y}$ ;  $\mathbf{X}' = \Sigma^{-1/2} \mathbf{X}$ 
6:    $\beta \leftarrow LASSO(\mathbf{Y}', \mathbf{X}')$ 
7:   for  $k = 1$  to  $p$  do
8:     calculate  $(\nabla g(\gamma))_k$ 
9:     update  $\gamma_k \leftarrow S_{\lambda_2 t}(\gamma_k - t \nabla g(\gamma_k))$ 
10:    update  $\Sigma$ 
11:   end for
12:   calculate the gradient for  $\tau_0$ :  $\frac{\partial L}{\partial \tau_0}$ 
13:   update  $\tau_0 \leftarrow \tau_0 - t \frac{\partial L}{\partial \tau_0}$ 
14:   update the loss function  $L$  with Equation 4
15:   if update for the loss function  $L$  in the iteration  $< \epsilon$  then
16:     break
17:   end if
18: end for

```

---

### 3.2 Model selection

For the model selection process, we use a strategy to fine-tune the parameters  $\lambda_1$  and  $\lambda_2$  to strike an optimal balance between model simplicity and performance.

- Fixing  $\lambda_2$ : We begin by setting  $\lambda_2$  to a fixed value, which controls the degree of regularization for variance shifts. With  $\lambda_2$  fixed, we focus on adjusting  $\lambda_1$ , which regulates the penalization of shifts in the optimal values.
- Cross-validation for  $\lambda_1$ : For each fixed value of  $\lambda_2$ , we use cross-validation to find the best  $\lambda_1$ . We use the `cv.glmnet` function from the R package `glmnet` to efficiently perform cross-validation here. We use cross-validation because `cv.glmnet` allows for quick and easy computation of cross-validation results, making it more convenient and efficient for selecting the optimal parameters.
- Iterating over different  $\lambda_2$  values: After optimizing  $\lambda_1$  for one fixed  $\lambda_2$ , we repeat this

process for multiple values of  $\lambda_2$ , producing a set of candidate models, each associated with different pairs of  $\lambda_1$  and  $\lambda_2$ .

- Selecting the best model using BIC: To identify the optimal model, we compare all candidate models across the range of  $\lambda_2$  values by using the Bayesian Information Criterion (BIC). The model with the lowest BIC is selected as the final model, as it achieves the best trade-off between goodness of fit and model complexity, minimizing the risk of overfitting.

We choose BIC over other criteria based on empirical findings in Zhang et al. [2024], where pBIC was found to be a more conservative criterion. While a conservative selection method can be beneficial in some cases, detecting shifts in variance is inherently more challenging than detecting shifts in optimal values. A less conservative criterion like BIC is preferable here, as it increases sensitivity to shifts in variance while still penalizing overly complex models. Additionally, BIC offers a computational advantage over pBIC.

## 4 Simulations

### 4.1 Comparison of performance

In the main simulation settings, we set  $\alpha = 1$  and the original variance  $\sigma_0^2 = 2$ . These parameter choices represent a moderate level of phylogenetic signal and baseline trait variance. For each parameter setting, we conducted 50 simulations. To assess the robustness of our conclusions, we also conducted additional simulations with different values of  $\alpha$ , which are provided in the supplementary materials. The results of these additional simulations are consistent with the main findings presented here. In the following simulations,  $\alpha$  is assumed to be unknown. For ShiVa, we obtain  $\alpha$  by fitting a null model (without shifts) using the `phylolm` package.

We compared the performance of different methods based on three key metrics: True Positives (TP), False Positives (FP), predictive log-likelihood, and computational time. Here, True Positives (TP) refer to the number of true shifts correctly detected, while False Positives (FP) refer to the number of false shifts incorrectly detected. However, the positions of shifts are not always identifiable—for example, under a 3-branch tree, any two shifts can lead to an identical model. In such cases, TP and FP may not be reliable metrics, as they would count the true model as including one false positive and missing one true positive, even though the models are effectively equivalent. Figure 3 illustrates the TP and FP results across the various methods under different scenarios. When there is only a shift in the optimal value, ShiVa achieves a well-balanced trade-off between True Positives and False Positives. It effectively detects shifts in the optimal value without generating excessive False Positives. The performance of ShiVa is comparable to other methods that only consider shifts in the optimal value even if only shift in optimal value is present. In contrast, PCMFit produces a much higher number of False Positives, particularly when the signal size is small.

In the case of shifts in variance, ShiVa performs well in detecting variance shifts effectively while maintaining control over False Positives. Although PCMFit shows a higher True Positive rate compared to ShiVa, it comes at the cost of generating significantly more False Positives. Methods like  $\ell_1$ ou and phyloEM, which are designed to detect shifts in optimal value, face challenges when a shift in variance is present. As the magnitude of the variance shift increases, these methods incorrectly interpret the variance signal as multiple shifts in the optimal value. Consequently, their False Positives increase substantially. In contrast, ShiVa successfully distinguishes between variance and mean shifts, effectively controlling the False Positive rate for optimal value shifts, even as the variance shift signal strengthens.

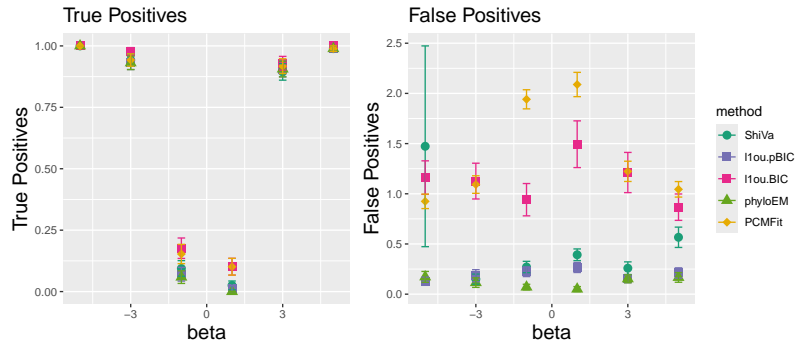
When both shifts in optimal value and variance are present, ShiVa continues to perform competitively. Although it detects slightly fewer True Positives compared to PCMFit,

its False Positive rate is much lower, indicating a better balance between sensitivity and specificity. PCMFit, while capable of identifying more shifts overall, tends to produce excessive False Positives. This leads to reduced reliability in shift detection, especially in noisy data.

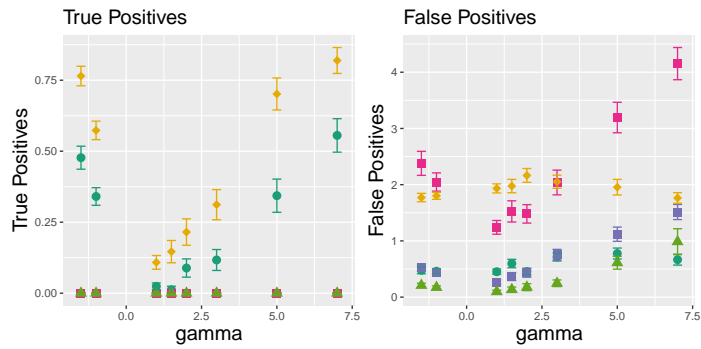
In addition to TP and FP, we also evaluated predictive log-likelihood to assess the prediction accuracy of the models estimated by different methods. Regarding identifiability, the OU model is identifiable when no shifts are present. However, previous studies have shown that the exact number and locations of shifts along an edge cannot always be fully determined due to identifiability issues. For example, any two of the three branches connected to a node can yield equivalent models. Even if the selected shifts do not match the true model exactly, choosing a close surrogate shift may be preferable to missing the shift entirely. In such cases, the true positive versus false positive framework might misrepresent performance: a method selecting a surrogate shift is penalized with a false positive, even though it provides a more reasonable approximation than failing to detect the shift. Predictive log-likelihood addresses this issue by evaluating how well the selected models predict new data. For each simulation, we generate 1,000 test datasets for each of the 2,000 simulated datasets, using the same tree and shift configurations. We then compute the mean log-likelihood across the 1,000 test datasets based on the estimated shifts from the training sets. Figure 4 illustrates the differences in predictive log-likelihood between the estimated models and the true model. When shifts occur only in optimal value, ShiVa performs comparably to  $\ell1ou$  and phyloEM, demonstrating similar predictive precision. However, when shifts in variance are introduced, ShiVa shows a notable improvement, achieving higher predictive log-likelihood than the other methods. In contrast, PCMFit consistently exhibits the lowest predictive log-likelihood across all scenarios, likely due to overfitting.

Finally, we compare the average computational time across different methods. Methods that only account for shifts in optimal values, such as  $\ell1ou$ , are the fastest, with  $\ell1ou$  be-

# DETECTION OF SHIFTS IN VARIANCE



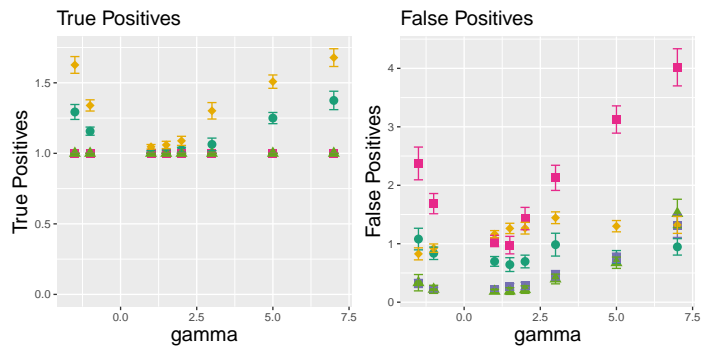
(a) 1 shift in optimal value



(b) 1 shift in variance



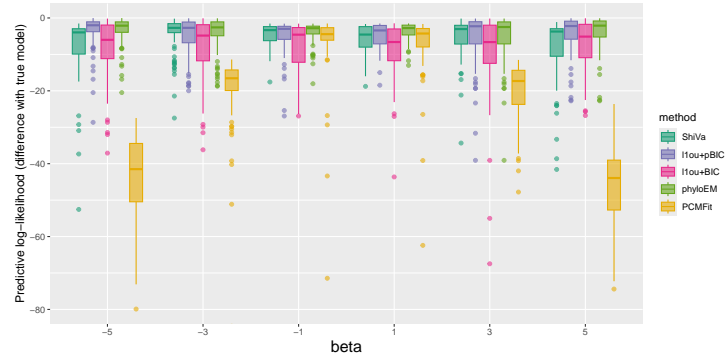
(c) 1 shift in optimal value + 1 shift in variance (fixed  $\gamma$ )



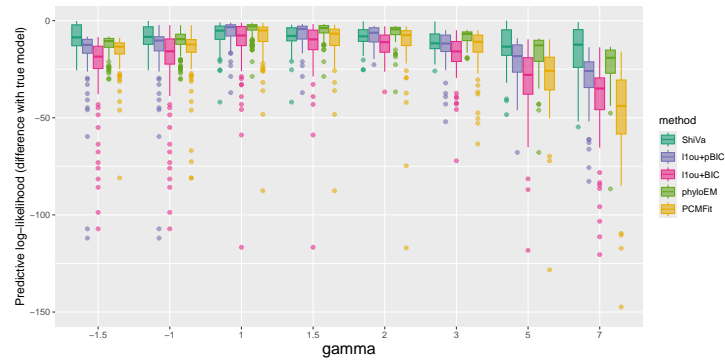
(d) 1 shift in optimal value + 1 shift in variance (fixed  $\beta$ )

Figure 3: Comparison of True positives and False positives of different methods

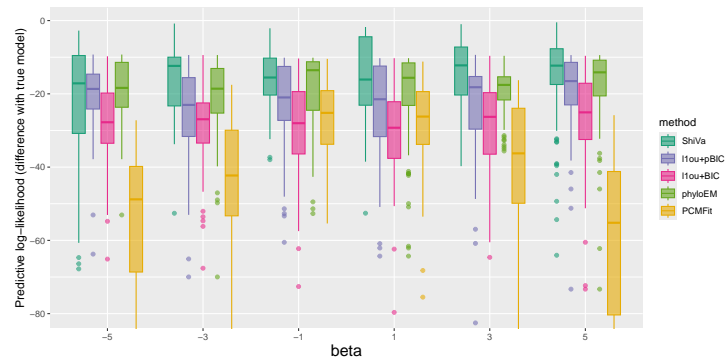
# DETECTION OF SHIFTS IN VARIANCE



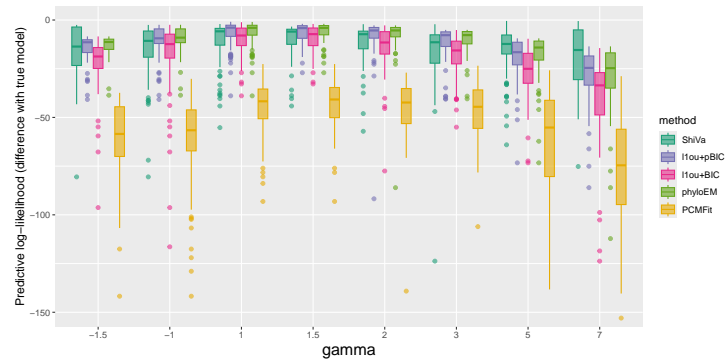
(a) 1 shift in optimal value



(b) 1 shift in variance



(c) 1 shift in optimal value + 1 shift in variance (fixed gamma)



(d) 1 shift in optimal value + 1 shift in variance (fixed beta)

Figure 4: Comparison of predictive log-likelihood of different methods

ing particularly efficient due to its use of the LASSO path method. ShiVa performs similarly to phyloEM but is slightly slower in comparison. On the other hand, PCMFit requires significantly more time due to its handling of complex computations, especially when both shifts in optimal values and variance are present. The current PCMFit implementation allows parallel computing to partially compensate for the disadvantage of the method in terms of computational complexity. For the comparisons in Table 1, we ran all methods single-threaded to provide a fairer comparison of computation required by all methods.

Table 1: Computational Time Comparison for Different Methods

Shift Position (mean)	Beta	Shift Position (variance)	Gamma	Average Computation Time				
				ShiVa	l1ou-pBIC	l1ou-BIC	phyloEM	PCMFit
71	1	0	0	95.38	8.09	8.31	68.15	11484.33
71	3	0	0	77.39	8.29	8.57	70.10	13592.56
71	5	0	0	73.86	8.59	8.78	69.92	12227.06
71	-1	0	0	143.39	7.86	8.24	67.81	12890.20
71	-3	0	0	75.70	8.31	8.45	70.02	16215.21
71	-5	0	0	70.33	8.37	8.57	69.35	11962.69
0	0	195	1	70.22	8.08	8.30	68.63	15171.28
0	0	195	1.5	83.31	8.08	8.42	67.72	15680.57
0	0	195	2	77.95	8.04	8.32	70.84	20622.02
0	0	195	3	87.73	8.52	8.81	70.93	16349.04
0	0	195	5	90.05	8.10	8.34	67.70	17358.66
0	0	195	7	97.68	8.18	8.53	67.85	19644.00
0	0	195	-1	101.92	8.04	8.30	67.95	15269.57
0	0	195	-1.5	102.83	7.58	7.74	65.42	15557.74
71	5	195	5	79.32	8.30	8.68	68.18	22836.10
71	3	195	5	129.45	8.55	8.73	68.68	24499.03
71	1	195	5	75.43	8.26	8.92	69.12	18023.39
71	-1	195	5	85.47	7.93	8.24	69.71	19622.12
71	-3	195	5	68.37	7.88	8.51	69.10	24580.25
71	-5	195	5	77.10	7.89	8.21	70.45	23177.43
71	5	195	1	76.73	8.23	8.53	70.06	16574.76
71	5	195	1.5	72.93	8.27	8.59	69.33	13153.55
71	5	195	2	76.58	8.18	8.61	68.71	15742.43
71	5	195	3	90.45	8.17	8.54	69.52	22800.45
71	5	195	7	87.67	8.42	8.67	69.44	23418.19
71	5	195	-1	92.83	8.23	8.45	70.31	16642.62
71	5	195	-1.5	95.15	8.31	8.51	70.79	17517.06

## 4.2 Relationship between shift position and detection difficulty

To investigate the difficulty of detecting shifts at specific positions on a phylogenetic tree, we conducted simulations for every internal branch of the tree. For each branch, we performed 50 simulations where a shift in the optimal value occurred and 50 simulations where a shift in variance occurred. We then calculated the detection probabilities for each shift using ShiVa, considering different positions on the tree. Figure 5 presents the detection probabilities for various branches, highlighting the different detection patterns for shifts in optima versus shifts in variance.

The results indicate that shifts in optima and shifts in variance exhibit distinct detection patterns. For shifts in the optimal value, those occurring near the root or the tips are easier to detect compared to shifts occurring in the middle regions of the tree. In contrast, shifts in variance are generally harder to detect. Our findings show that shifts in variance are more likely to be detected when they occur on branches with a larger number of descendant tips and longer branch lengths, which provides a stronger signal for the variance change. This pattern aligns with our analysis in the *Evolutionary shifts in optimal value and variance* subsection. The overall results emphasize the importance of the tree structure and branch characteristics in determining the detectability of evolutionary shifts, with shifts in variance requiring more stringent conditions for reliable detection compared to shifts in optima.

## 4.3 The influence of estimation of $\alpha$

We conducted simulations to investigate how the misestimation of  $\alpha$  affects ShiVa's shift detection results. In these simulations, we set the true value of  $\alpha$  to 1 (corresponding to  $\log(\alpha) = 0$ ). To assess the impact of different levels of misestimation, we tested a range of estimated  $\alpha$  values, using  $\log(\alpha) = -5, -3, -1, 0, 1, 3, 5$  as inputs to the ShiVa function. The detection results were evaluated by comparing the predictive log-likelihoods across these different estimated values of  $\alpha$ .

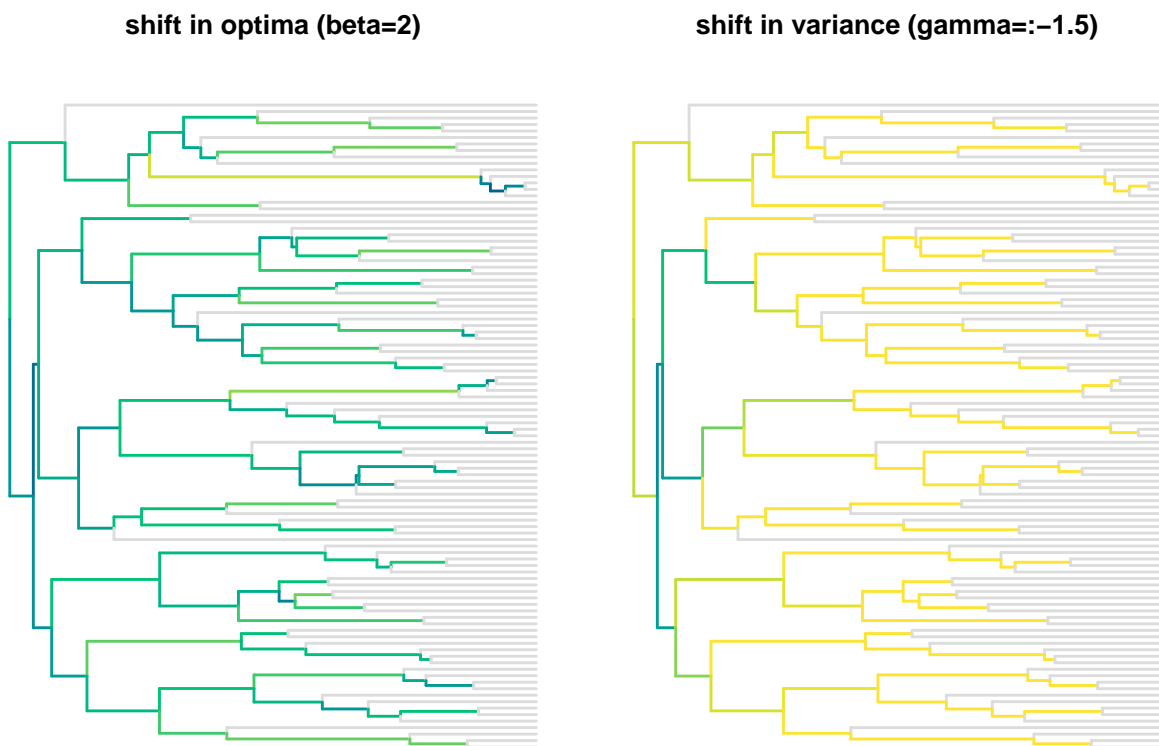
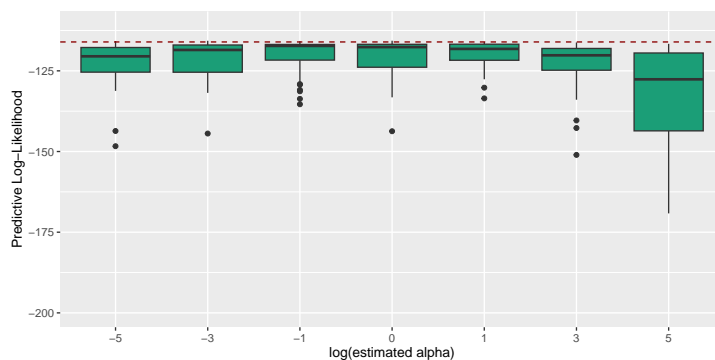
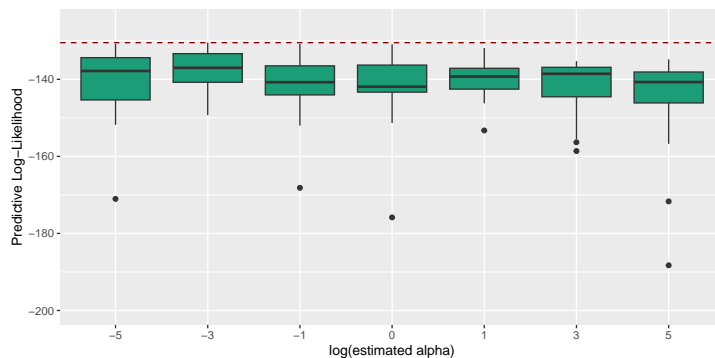


Figure 5: The detection probability of a shift on different branches (ShiVa)

For this analysis, we focused on scenarios with one shift in the optimal value and one shift in variance, representing a typical use case for ShiVa. The results suggest that, in most cases, moderate misestimation of  $\alpha$  has little effect on ShiVa’s performance. However, the impact becomes more pronounced in extreme cases — particularly when the estimated  $\alpha$  is very large (e.g.,  $\exp(5)$ ) and the shift signal size is also very large. This indicates that while ShiVa is generally robust to  $\alpha$  misestimation, severe overestimation combined with strong signals may reduce detection accuracy. Overall, this analysis supports the practical simplification of using a reasonable ad-hoc estimate of  $\alpha$  in applications.



(a) 1 shift in optimal value:  $\beta = 3$



(b) 1 shift in variance:  $\gamma = 3$

Figure 6: Comparison of predictive log-likelihood of ShiVa with different estimation of  $\alpha$

#### 4.4 The effect of shift position within a branch

In *Trait evolution with shifts in both optimal value and variance*, we noted that our assumptions about the shifts in variance—at most one shift will occur on any branch; and

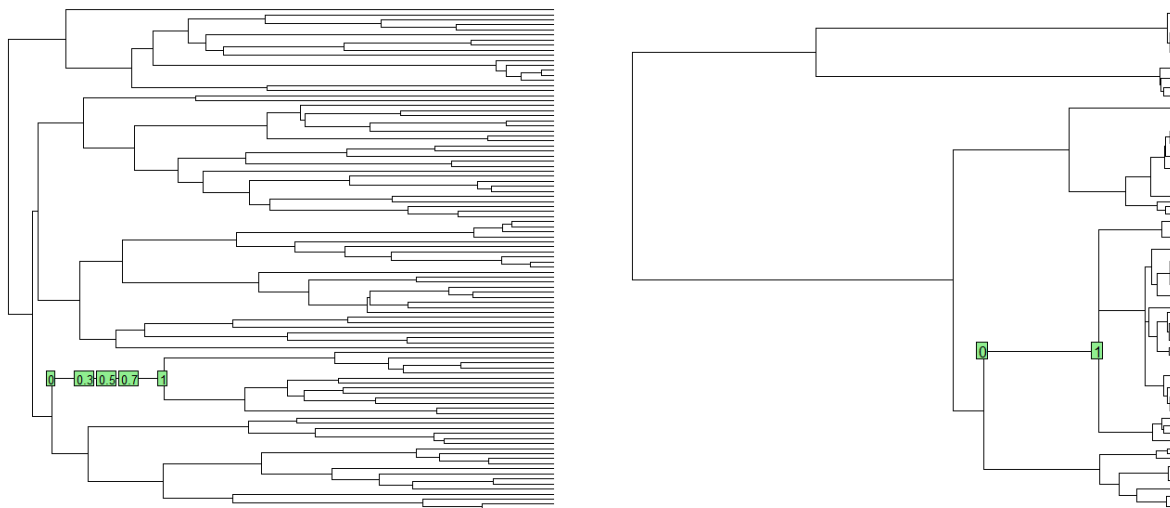


Figure 7: Left: The different locations of shifts on the same branch; Right: Two opposite shifts occur on the same branch

the shifts occur at the beginning of the branches—are restrictions on the space of possible models, so in particular if these assumptions are not satisfied, then the model is misspecified. In this subsection, we conduct simulations in which these assumptions are violated. Firstly, we conduct a series of simulations with the shift occurring in different positions along a fixed branch. The different locations of the shift are shown in Figure 7 (left). Figure 8 shows the True Positives v.s. False Positives rates and the predictive log-likelihood difference between ShiVa and the true model with shifts in different locations. Location here is a parameter ranging from 0 to 1, with 0 meaning the beginning of the branch and 1 meaning the end of the branch. The ability of the method to detect the shift in variance is not greatly impacted by the position of the shift along the branch. Furthermore, when the shift size is small, the log-likelihood of the model is not much reduced in situations where the location of the shift is not at the beginning of the branch. However, when the magnitude of the shift is larger, the model misspecification does cause a substantial decrease in log-likelihood when the shift is not located at the beginning of the branch. Overall, our method is robust to violations of our assumption that shifts occur at the beginning of a branch.

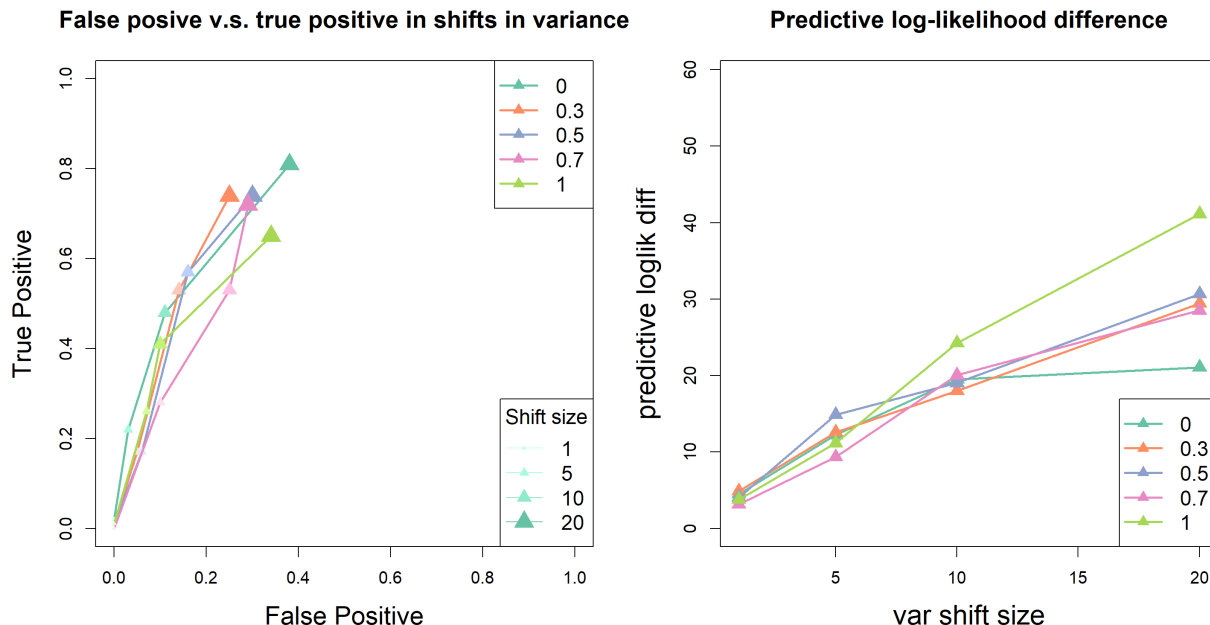


Figure 8: The true positive v.s. false positive rates and the predictive log-likelihood difference of ShiVa with shifts at different locations

Secondly, we simulate scenarios with two shifts on a single branch. If shifts are both positive or both negative, the data will show a stronger signal than when just one shift occurs. Therefore, we simulate situations where two opposite shifts occur (at locations = 0 and 1) (Figure 7 right). To compare, we also simulate situations where only one shift occurs at the beginning of that branch. Table 2 shows that when the two opposite shifts occur on that branch, our method cannot accurately detect the shift in variance on that branch and the false positive rate of shifts in optimal value increases. In this case, the violation of the assumption causes some difficulties for our method. However, in the general case, it is not a major concern.

## 5 Case study: Cordylid data

*Cordylidae* is a family of lizards in Sub-Saharan Africa (Stanley, Bauer, Jackman, Branch, and Mouton, 2011). Broeckhoven et al. [2016a] selected 28 species of *Cordylidae*, including

Table 2: The performance of ShiVa when two opposite shifts occur on the same branch

Shift Size		20	15	10	5	1
False positive(optimal value)	opposite shifts	0.66	0.63	0.49	0.48	0.44
	single shift	0.4	0.5	0.26	0.49	0.43
True positive(variance)	opposite shifts	0	0	0	0	0
	single shift	0.9	0.86	0.84	0.41	0.01
False positive(variance)	opposite shifts	0.01	0	0.02	0	0
	single shift	0.73	0.7	0.57	0.21	0.02

five outgroup taxa, and reconstructed the phylogenetic tree based on their DNA sequences using BEAST. They also collected 20 morphological traits, including spine, limb and head dimensions and used pPCA (Revell, 2009) to perform dimension reduction. Based on their analysis, the first principal component pPCA1 represented a gradient from highly armored species to lightly armored species. The phylogenetic tree and principal component data are available in the R package phytools: <http://www.phytools.org/Rbook/>. We used the cordylid tree and the first principal component they provided to compare the shift detection results of  $\ell_{1ou}$ , phyloEM and ShiVa.

Figure 9 shows the results given by different methods. ShiVa uses cross validation to tune the hyperparameter  $\lambda_1$ , therefore the final results have randomness. We repeat the method 3 times and select the best model based on BIC for this real data analysis. The model estimated by ShiVa gives the highest log-likelihood (18.2) and the lowest BIC (40.24).

$\ell_{1ou}+pBIC$  and phyloEM detected limited numbers of shifts, with lower log-likelihood and higher BIC compared to the other two methods. Comparing the results of  $\ell_{1ou}+BIC$  and ShiVa,  $\ell_{1ou}+BIC$  detected branches 28, 43, 44 as shifts in optimal value, and ShiVa detected a shift in variance: branch 47, without detecting the above shifts in optimal value. From the results of ShiVa, it is possible that the subgroup *Cordylus* has a different variance from other taxa. This interesting finding may be neglected, and indeed detected as

multiple false shifts in optimal values using the other methods.

To determine which of the shifts in optimal value and variance selected by the various methods are more plausible, we simulated 100 datasets based on each selected model and applied  $\ell_{1ou}$ , phyloEM and ShiVa to check whether the models selected by the different methods are plausible for this combination of true shifts. Table 3 shows the validation results. If the models selected by  $\ell_{1ou}+pBIC$  or by phyloEM were true, then it is very unlikely that  $\ell_{1ou}+BIC$  or ShiVa would detect as many shifts as they do for the real data. Similarly, if the model selected by  $\ell_{1ou}+BIC$  were true, it would be unlikely that ShiVa would select so many shifts in variance. On the other hand, the results for the simulation based on the shifts identified by ShiVa are more similar to the real data results. Figure 11 shows more detailed results from these simulations. We see that in terms of the total number of shifts selected in both optimal value and variance, the simulation results for the model selected by ShiVa are far more similar to the real data. This suggests that this model is more likely to be close to the truth. We see that ShiVa often selects surrogates to the true shifts in simulations, so we cannot be confident of the exact location of the shifts, but it certainly appears that there are shifts in variance, and these shifts have impacted the performance of shift detection methods that only detect shifts in optimal value. The shifts in optimal value detected by these methods, but not by ShiVa are likely to be false positives caused by the shifts in variance.

Considering the log-likelihood, BIC, and the validation results, the shifts in optimal value and variance detected by ShiVa in the cordylid dataset fit the data better compared to other methods.

## 6 Conclusion

In this article, we have used a multi-optima multi-variance OU process to describe an evolutionary process where abrupt shifts can occur in either optimal value or variance. We

# DETECTION OF SHIFTS IN VARIANCE

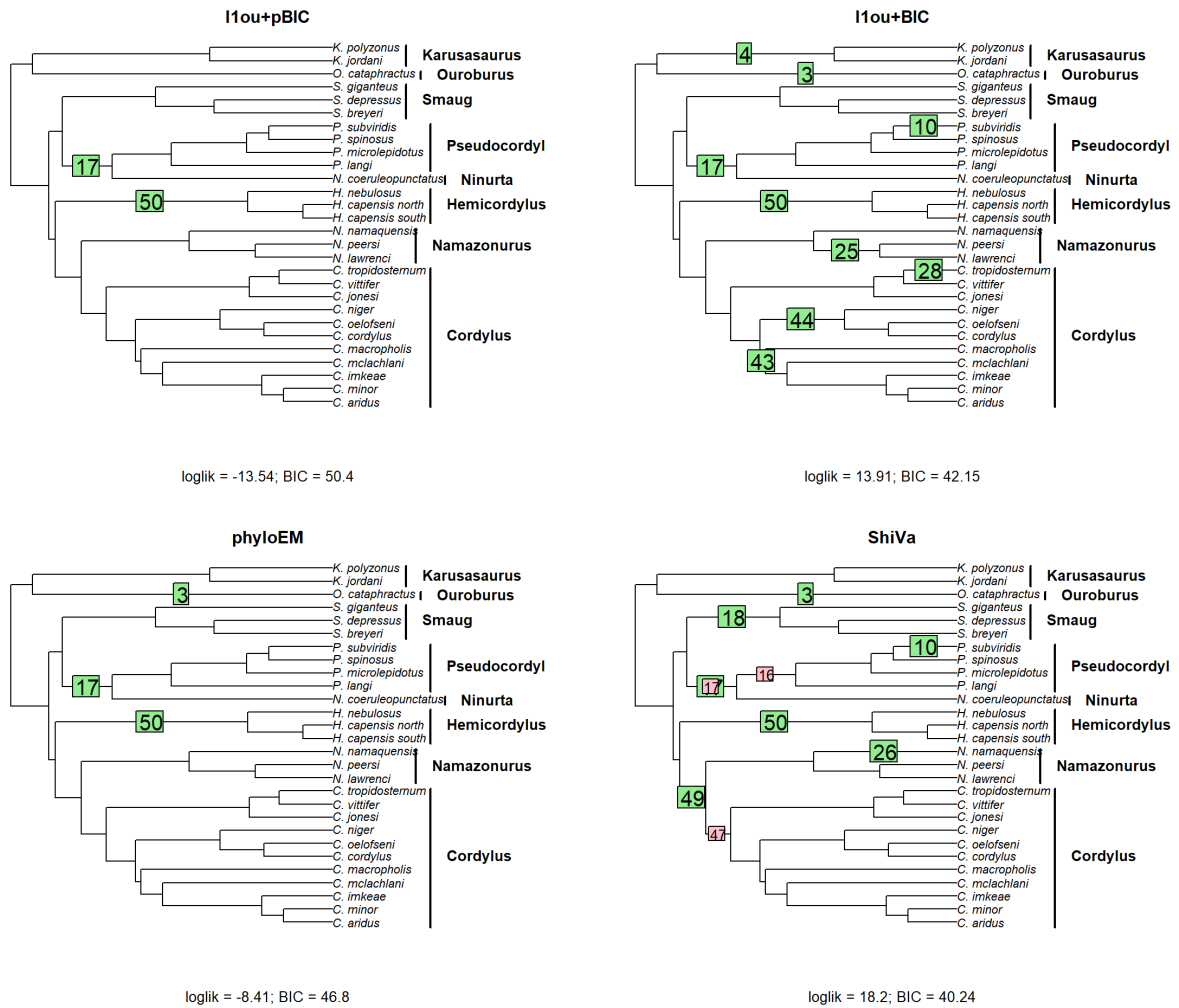


Figure 9: The shift detection results of cordylid data of  $\ell_{1ou+pBIC}$  (left top),  $\ell_{1ou+BIC}$  (right top), phyloEM (left bottom) and ShiVa (right bottom)

Table 3: True positive versus False positive rates of different methods using data simulated from the estimated model given by Figure 9

Model simulated from	Shifts in optimal value	Shifts in variance	Method	True positive (optimal value)	False positive (optimal value)	True positive (variance)	False positive (variance)
l1ou_pBIC	17;50		ShiVa	2.00	0.24	0.00	0.63
			l1ou+pBIC	2.00	0.05	0.00	0.00
			l1ou+BIC	2.00	4.80	0.00	0.00
			phyloEM	2.00	0.13	0.00	0.00
l1ou_BIC	3;4;10;17;25;28;43;44;50		ShiVa	3.43	0.87	0.00	0.14
			l1ou+pBIC	2.32	0.01	0.00	0.00
			l1ou+BIC	7.18	3.67	0.00	0.00
			phyloEM	3.53	1.19	0.00	0.00
phyloEM	3;17;50		ShiVa	2.62	1.16	0.00	0.71
			l1ou+pBIC	2.39	0.05	0.00	0.00
			l1ou+BIC	2.87	5.62	0.00	0.00
			phyloEM	2.65	0.20	0.00	0.00
ShiVa	3;10;17;18;26;49;50	16;17;47	ShiVa	5.94	3.08	0.40	0.82
			l1ou+pBIC	1.50	0.02	0.00	0.00
			l1ou+BIC	5.72	6.56	0.00	0.00
			phyloEM	3.48	0.78	0.00	0.00

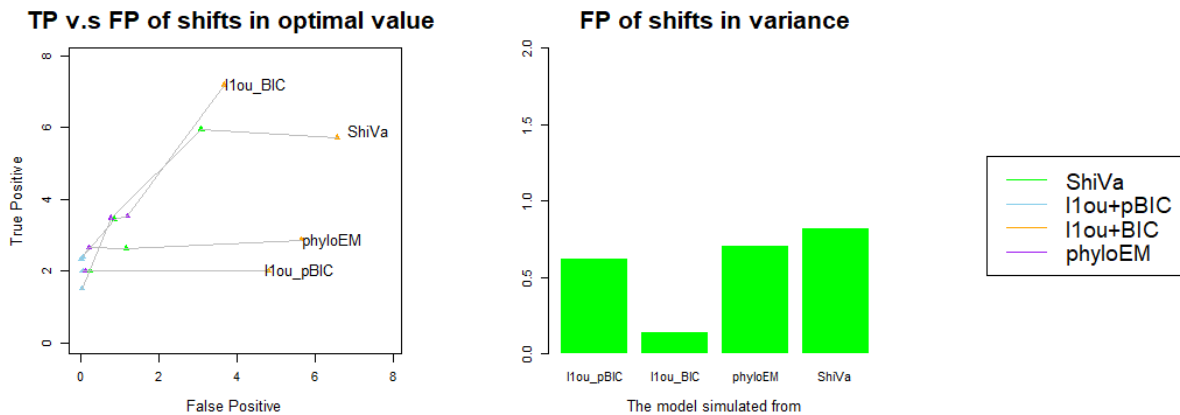


Figure 10: Left: True positive versus false positive rates of the shifts in optimal values detected by different methods. Right: False positive rates of the shifts in variance detected by ShiVa.



Figure 11: The selecting frequencies of shifts given by different methods; deeper color shows higher selecting frequency. (Green: selecting frequencies of shifts in optimal value; Red: selecting frequencies of shift in variance). The row names show the model data are simulated from; the column names show the method applied to the generated data. The asterisk marks show the true shifts of the model that the data are simulated from.

then proposed a new method to simultaneously detect shifts in optimal value and shifts in variance. We implemented the method in R. Our package is available from the first author's GitHub page <https://github.com/WenshaZ/ShiVa>. Furthermore, we have conducted simulation studies to show the effectiveness of our method to detect both kinds of shifts and compared it to methods which only detect shifts in optimal value.

Our results showed that ShiVa effectively balances True Positives (TP) and False Positives (FP) across different scenarios. When there was only a shift in the optimal value, ShiVa performed comparably to other methods, such as  $\ell$ 1ou and phyloEM, maintaining similar predictive accuracy while achieving a better balance between TP and FP compared to PCMFit, which tended to overfit in weak signal scenarios. When a shift in variance was present, ShiVa demonstrated a significant advantage over other methods, achieving higher predictive log-likelihood and effectively distinguishing between variance and mean shifts. This led to fewer False Positives compared to  $\ell$ 1ou and phyloEM, which often misinterpreted variance shifts as multiple shifts in optimal value. Although PCMFit achieved higher TP rates, it generated significantly more FP, indicating overfitting.

We applied our method to the first principal component of trait values for the cordylid data from Broeckhoven et al. [2016a]. ShiVa detected 7 shifts in optimal value and 3 shifts in variance and the model given by ShiVa has the highest log-likelihood and lowest BIC compared to  $\ell$ 1ou and phyloEM. The validation result also shows that ShiVa would be unlikely to estimate the model it did if any of the models selected by other methods were true.

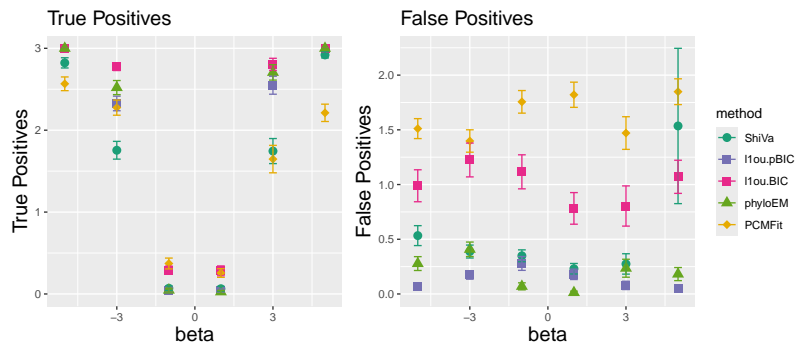
For model simplicity, we assume that the variance parameter is constant along each branch and that all shifts in variance happen at the beginning of the branch. Simulations of cases where these assumptions are violated show that our method is robust to misspecification in these assumptions. An interesting future research direction is to extend our model to allow shifts in variance at internal positions along a branch. This would allow us to estimate the exact time of a shift in variance. Writing the likelihood for this case is straightforward,

but more work may be needed to ensure stability of the estimates. Another direction for future work is to improve the computational efficiency of the method. The likelihood calculation involves a large number of matrix inverse computations, which can be computationally expensive for large trees. Bastide et al. [2021] provide an efficient algorithm to calculate the log likelihood and its derivatives for certain phylogenetic models. If this method could be adapted to our method, it would lead to a major improvement in the computational speed, allowing our method to scale to larger phylogenies.



# A Supplemental Materials

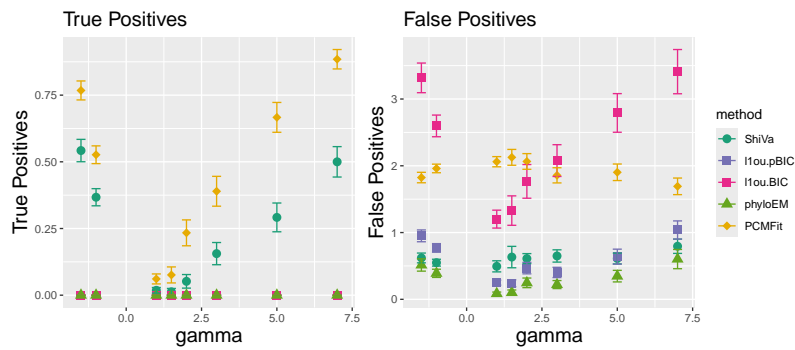
f



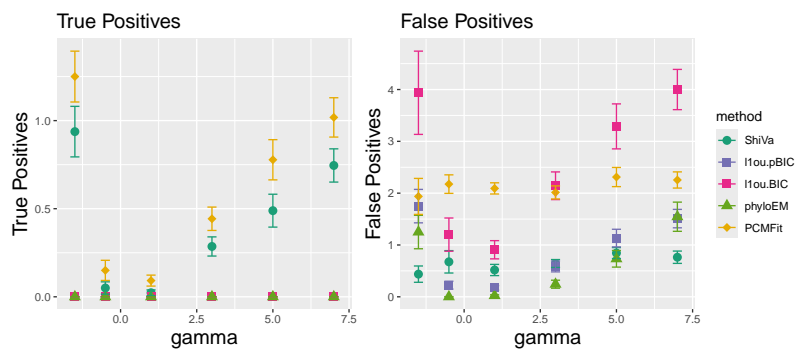
(a) 3 shifts in optimal value



(b) 7 shifts in optimal value

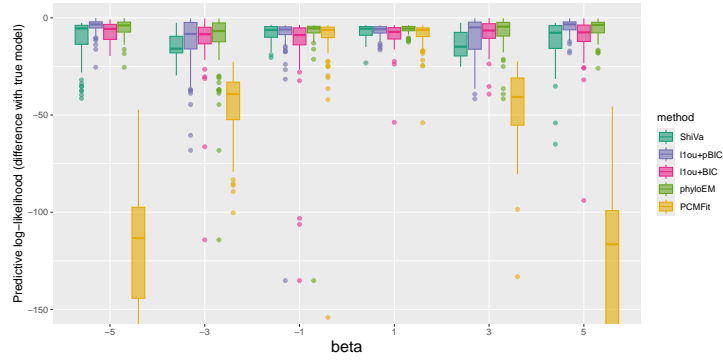


(c) 1 shift in variance (different position)

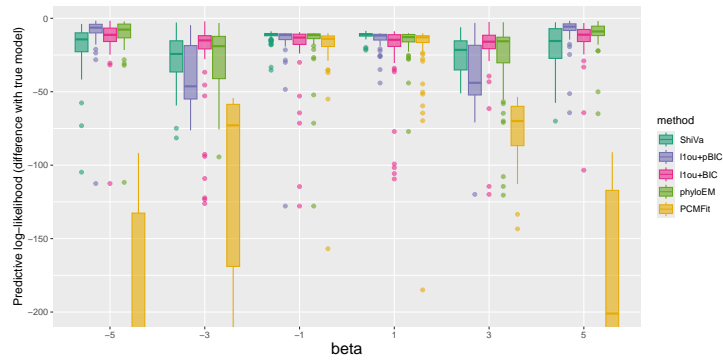


(d) 2 shifts in variance

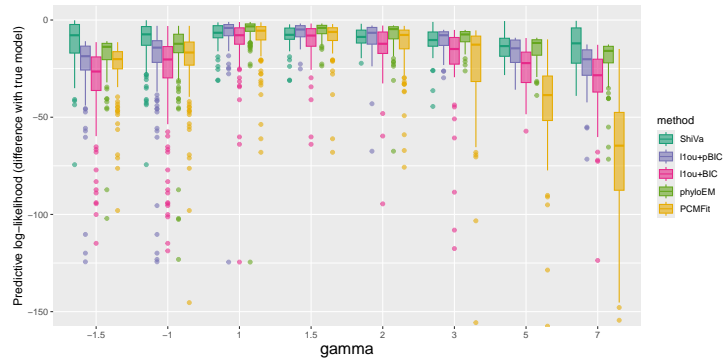
Figure 12: Comparison of True positives and False positives of different methods (Supplementary simulations)



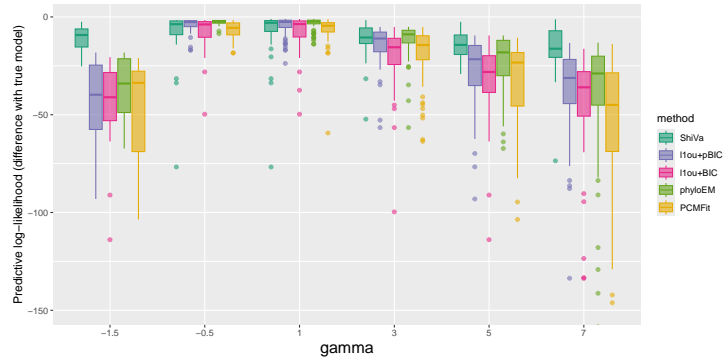
(a) 3 shifts in optimal value



(b) 7 shifts in optimal value



(c) 1 shift in variance (different position)



(d) 2 shifts in variance

Figure 13: Comparison of predictive log-likelihood (difference with true model) of different methods (Supplementary simulations)

## B Data accessibility

The tree of Anolis lizards is provided by Mahler et al. [2013b]. It can be found in the Dryad data repository: <https://doi.org/10.5061/dryad.9g182>. The phylogenetic tree and principal component data of cordylid data (Broeckhoven, Diedericks, Hui, Makhubo, and Mouton, 2016b) can be found in the Dryad data repository: <https://doi.org/10.5061/dryad.k186f>. Our R package is available at <https://github.com/WenshaZ/ShiVa>.

## C Author contributions

All authors contributed to conceive the ideas, design the methodology and the simulations. WZ conducted the simulations, analyzed the results and wrote the manuscript under the guidance of LSTH and TK. LSTH and TK reviewed and edited the manuscript.

## D Acknowledgement

LSTH was supported by the Canada Research Chairs program, the NSERC Discovery Grant RGPIN-2018-05447, and the NSERC Discovery Launch Supplement. TK was supported by the NSERC Discovery Grant RGPIN/4945-2014.

## Bibliography

Paul Bastide, Mahendra Mariadassou, and Stéphane Robin. Detection of adaptive shifts on phylogenies by using shifted stochastic processes on a tree. *Journal of the Royal Statistical Society: Series B (Statistical Methodology)*, 79(4):1067–1093, 2017. doi: 10.1111/rssb.12206.

Table 4: Computational Time Comparison for Different Methods (Supplementary simulations)

Shift Position (mean)	Beta	Shift Position (variance)	Gamma	Average Computation Time				
				ShiVa	l1ou-pBIC	l1ou-BIC	phyloEM	PCMFIt
43,71,192	1	0	0	86.80	7.66	8.43	69.64	11561.58
43,71,192	3	0	0	74.95	8.37	8.36	68.09	27477.04
43,71,192	5	0	0	88.87	8.76	8.86	68.05	36900.89
43,71,192	-1	0	0	71.88	7.99	8.40	69.21	13952.25
43,71,192	-3	0	0	67.89	8.61	8.56	70.58	35867.14
43,71,192	-5	0	0	76.54	9.13	9.16	72.69	40202.81
6,71,197,3,88,191,98	1	0	0	117.94	7.80	8.05	70.53	14863.06
6,71,197,3,88,191,98	3	0	0	80.94	6.06	6.08	70.63	31135.83
6,71,197,3,88,191,98	5	0	0	81.68	8.55	8.86	67.94	59322.66
6,71,197,3,88,191,98	-1	0	0	83.20	7.79	8.04	69.02	15652.61
6,71,197,3,88,191,98	-3	0	0	98.53	7.42	6.84	69.47	29763.69
6,71,197,3,88,191,98	-5	0	0	69.55	7.99	7.85	70.15	60076.49
0	0	196	1	68.06	8.08	8.35	69.46	14515.10
0	0	196	1.5	72.20	8.03	8.31	69.51	15649.65
0	0	196	2	83.65	8.39	8.54	70.18	17266.36
0	0	196	3	90.27	7.61	8.14	69.24	18907.37
0	0	196	5	89.08	8.27	8.42	69.61	18364.71
0	0	196	7	101.44	8.03	8.51	67.09	18858.03
0	0	196	-1	99.09	8.26	8.66	67.89	16773.86
0	0	196	-1.5	113.54	8.21	8.72	67.30	19419.61
0	0	195,130	1,-0.5	80.75	8.37	8.68	70.94	16275.18
0	0	195,130	3,-1	93.39	8.11	8.39	70.21	18297.14
0	0	195,130	5,-1.5	159.13	12.06	12.58	116.55	36602.57
0	0	195,130	7,-1.5	114.15	8.60	8.86	69.08	22939.48
0	0	195,130	1	85.99	8.15	8.31	70.17	15881.60
0	0	195,130	3	91.66	8.10	8.38	70.03	17969.21
0	0	195,130	5	104.25	8.69	9.17	71.10	25327.97
0	0	195,130	7	95.08	8.63	8.94	69.17	23545.64

- Paul Bastide, Lam Si Tung Ho, Guy Baele, Philippe Lemey, and Marc A. Suchard. Efficient bayesian inference of general gaussian models on large phylogenetic trees. *The Annals of Applied Statistics*, 15(2), 2021. doi: 10.1214/20-aoas1419.
- Jeremy M. Beaulieu, Dwueng-Chwuan Jhwueng, Carl Boettiger, and Brian C. O’Meara. Modeling stabilizing selection: Expanding the ornstein-uhlenbeck model of adaptive evolution. *Evolution*, 66(8):2369–2383, 2012. doi: 10.1111/j.1558-5646.2012.01619.x.
- Chris Broeckhoven, Genevieve Diedericks, Cang Hui, Buyisile G. Makhubo, and P. le Mouton. Enemy at the gates: Rapid defensive trait diversification in an adaptive radiation of lizards. *Evolution*, 70(11):2647–2656, 2016a. doi: 10.1111/evo.13062.
- [dataset] Chris Broeckhoven, Genevieve Diedericks, Cang Hui, Buyisile G. Makhubo, and Pieter le Fras Nortier Mouton. Data from: Enemy at the gates: rapid defensive trait diversification in an adaptive radiation of lizards, 2016b. Dryad. doi: 10.5061/dryad.k186f.
- Marguerite A. Butler and Aaron A. King. Phylogenetic comparative analysis: A modeling approach for adaptive evolution. *The American Naturalist*, 164(6):683–695, 2004. doi: 10.1086/426002.
- J. Clavel, G. Escarguel, and G. Merceron. mvmorph: An r package for fitting multivariate evolutionary models to morphometric data. *Methods in Ecology and Evolution*, 6(11): 1311–1319, 2015. doi: 10.1111/2041-210X.12420.
- Joseph Felsenstein. Phylogenies and the comparative method. *The American Naturalist*, 125(1):1–15, 1985. doi: 10.1086/284325.
- Thomas F. Hansen. Stabilizing selection and the comparative analysis of adaptation. *Evolution*, 51(5):1341, 1997. doi: 10.2307/2411186.
- Lam Si Tung Ho and Cécile Ané. Asymptotic theory with hierarchical autocorrelation:

- Ornstein–uhlenbeck tree models. *The Annals of Statistics*, 41(2), 2013. doi: 10.1214/13-aos1105.
- Lam Si Tung Ho and Cécile Ané. Intrinsic inference difficulties for trait evolution with ornstein-uhlenbeck models. *Methods in Ecology and Evolution*, 5(11):1133–1146, 2014. doi: 10.1111/2041-210x.12285.
- Mohammad Khabbazian, Ricardo Kriebel, Karl Rohe, and Cécile Ané. Fast and accurate detection of evolutionary shifts in ornstein–uhlenbeck models. *Methods in Ecology and Evolution*, 7(7):811–824, 2016. doi: 10.1111/2041-210x.12534.
- Jonathan B. Losos. *Lizards in an evolutionary tree: Ecology and adaptive radiation of anoles*. University of California Press, 2011.
- D. Luke Mahler, Travis Ingram, Liam J. Revell, and Jonathan B. Losos. Exceptional convergence on the macroevolutionary landscape in island lizard radiations. *Science*, 341(6143):292–295, 2013a. doi: 10.1126/science.1232392.
- [dataset] D. Luke Mahler, Travis Ingram, Liam J Revell, and Jonathan B. Losos. Data from: Exceptional convergence on the macroevolutionary landscape in island lizard radiations, 2013b. Dryad. doi: 10.5061/dryad.9g182.
- Venelin Mitov, Krzysztof Bartoszek, Georgios Asimomitis, and Tanja Stadler. Fast likelihood calculation for multivariate gaussian phylogenetic models with shifts. *Theoretical Population Biology*, 131:66–78, 2020. doi: 10.1016/j.tpb.2019.11.005.
- Mark Pagel and Andrew Meade. Bayesian analysis of correlated evolution of discrete characters by reversible-jump markov chain monte carlo. *The American Naturalist*, 167(6): 808–825, 2006. doi: 10.1086/503444.
- Neal Parikh and Stephen Boyd. Proximal algorithms. *Foundations and Trends in Opti-*

*mization*, 1(3):127–239, 2014. URL [https://web.stanford.edu/~boyd/papers/pdf/prox\\_algs.pdf](https://web.stanford.edu/~boyd/papers/pdf/prox_algs.pdf).

Liam J. Revell. Size-correction and principal components for interspecific comparative studies. *Evolution*, 63(12):3258–3268, 2009. doi: 10.1111/j.1558-5646.2009.00804.x.

Edward L. Stanley, Aaron M. Bauer, Todd R. Jackman, William R. Branch, and P. Le Mouton. Between a rock and a hard polytomy: Rapid radiation in the rupicolous girdled lizards (squamata: Cordylidae). *Molecular Phylogenetics and Evolution*, 58(1):53–70, 2011. doi: 10.1016/j.ympev.2010.08.024.

Josef C. Uyeda and Luke J. Harmon. A novel bayesian method for inferring and interpreting the dynamics of adaptive landscapes from phylogenetic comparative data. *Systematic Biology*, 63(6):902–918, 2014. doi: 10.1093/sysbio/syu057.

Wensha Zhang, Toby Kenney, and Lam Si Ho. Evolutionary shift detection with ensemble variable selection. *BMC Ecology and Evolution*, 24(1), Jan 2024. doi: 10.1186/s12862-024-02201-w.

## List of Figures

1	Higher original covariance between two species leads to larger change in covariance for the same shift magnitude: larger change for the shift in the left figure . . . . .	12
2	Earlier shift leads to larger change in covariance for a given species: larger change for the shift in the left figure . . . . .	12
3	Comparison of True positives and False positives of different methods . . . . .	20
4	Comparison of predictive log-likelihood of different methods . . . . .	21
5	The detection probability of a shift on different branches (ShiVa) . . . . .	24
6	Comparison of predictive log-likelihood of ShiVa with different estimation of $\alpha$ . . . . .	25
7	Left: The different locations of shifts on the same branch; Right: Two opposite shifts occur on the same branch . . . . .	26
8	The true positive v.s. false positive rates and the predictive log-likelihood difference of ShiVa with shifts at different locations . . . . .	27
9	The shift detection results of cordylid data of $\ell_{1ou+pBIC}$ (left top), $\ell_{1ou+BIC}$ (right top), phyloEM (left bottom) and ShiVa (right bottom) . . . . .	30
10	Left: True positive versus false positive rates of the shifts in optimal values detected by different methods. Right: False positive rates of the shifts in variance detected by ShiVa. . . . .	31

11	The selecting frequencies of shifts given by different methods; deeper color shows higher selecting frequency. (Green: selecting frequencies of shifts in optimal value; Red: selecting frequencies of shift in variance). The row names show the model data are simulated from; the column names show the method applied to the generated data. The asterisk marks show the true shifts of the model that the data are simulated from. . . . .	32
12	Comparison of True positives and False positives of different methods (Supplementary simulations) . . . . .	36
13	Comparison of predictive log-likelihood (difference with true model) of different methods (Supplementary simulations) . . . . .	37